Biomass Conversion and Biorefinery (2024) 14:9793–9803
https://doi.org/10.1007/s13399-023-03738-4

ORIGINAL ARTICLE

Valorization of orange peels in a biorefinery loop: recovery of limonene and production of volatile fatty acids and activated carbon

Fabio Rizzioli[1] · Vittoria Benedetti[2] · Francesco Patuzzi[2] · Marco Baratieri[2] · David Bolzonella[1] · Federico Battista[1]

Received: 25 October 2022 / Revised: 22 December 2022 / Accepted: 31 December 2022 / Published online: 13 January 2023

Abstract
Orange peels (OPs) were valorized in a lab-scale biorefinery loop for the recovery of limonene and the subsequent production of volatile fatty acids (VFAs) and activated carbon (AC). Solid/liquid extraction of limonene was optimized using *n*-hexane at 85 °C with an OPs-to-solvent ratio of 2:1, allowing for a limonene recovery yield of 1.20% w/w. Then, post-extraction OPs were used for the production of both VFAs and AC. For VFA production, a hydraulic retention time (HRT) of 5 days and a total solid (TS) inlet content of 10% w/w were adopted leading to a VFA yield of about 43% gVFAs/gTS. Adsorption tests revealed that, among all the solid matrixes tested, only powdered activated carbon (PAC) was able to discriminate no-VFA compounds and allowed for VFA purification. For AC production, post-extraction OPs were firstly converted into biochar through slow pyrolysis at 550 °C for 1 h and then physically activated with CO_2 at 880 °C for 1 h. Extraction did not appreciably affect OP properties, while pyrolysis increased the carbon content (from 43 to 83%) and the heating value (from 17 to 29 MJ/kg) of the material. Physical activation of OP biochar increased its surface area by almost ten times, from 40 to 326 m^2/g, proving the effectiveness of the treatment.

Keywords Orange peel · Biorefinery · Limonene · Volatile fatty acids · Activated carbon

1 Introduction

The European Commission adopted the new circular economy action plan (CEAP) in March 2020, one of the main building blocks of the European Green Deal, which aims at achieving climate neutrality by 2050, while promoting sustainable growth, minimizing waste, increasing resource efficiency, halting biodiversity loss, and fostering long-term competitiveness. The CEAP involves initiatives along the entire life cycle of products and services, encouraging the implementation of circular economy processes, the valorization of resources, and the reduction of waste generation. These objectives are also included in the Waste Framework Directive [1], the main legal EU document regulating the management of waste, which also defines the "waste hierarchy" concept based on the subsequent steps of prevention, reuse, recycling, recovery, and disposal. According to the waste hierarchy, wastes still containing valuable compounds should be recovered as "raw secondary materials" for the production of new goods through recycling. When recycling is not possible, waste can be further exploited for bioenergy production, while landfill disposal and incineration should be avoided, as they are considered less virtuous actions.

In this work, the waste hierarchy was adopted for the set-up of a lab-scale biorefinery, including different types of unit operations (biological, physical, thermal, and chemical), for the valorization of orange peels (OPs).

Around 70 Mtons of oranges are produced every year globally. At the European level, Italy Spain and Greece are the main producers with 6 Mtons of oranges produced every year [2]. The main by-product from the cultivation and consumption of this fruit is represented by OPs, which constitute up to 65% of total orange waste. OPs are often present in the Organic Fraction of Municipal Solid Waste (OFMSW), especially during the winter season, but the majority of OPs are collected after orange juice production in industrial

✉ Vittoria Benedetti
vittoria.benedetti@unibz.it

[1] Department of Biotechnology, University of Verona, Via Strada Le Grazie 15, 37134 Verona, Italy

[2] Faculty of Science and Technology, Free University of Bolzano, Piazza Università 1, 39100 Bolzano, Italy

plants, where oranges undergo the following unit operations to be transformed into soft drink: washing, grading, sorting, juice extraction and heat treatment [3].

Since the traditional management of OPs involves landfill disposal and incineration, non-virtuous practices according to the European Commission, in the last years, several works have focused on new processes for their valorization through the production of biofuels and high economic value bio-compounds: bioethanol, lactic acid [4], pectin and activated carbon [5], and biomethane by anaerobic digestion [6]. In particular, OPs have been receiving great attention due to their high concentration of limonene. Limonene is a cyclic monoterpene ($C_{10}H_{16}$), with two isomers, i.e., D- and L-limonene, smelling like orange and turpentine, respectively [7]. In particular, the oil extracted from oranges is essentially constituted by D-limonene [3]. Its chemical properties make limonene largely used as additive in different fields, especially as flavoring in the production of perfumes and body-care products, as reported by the EU document "Insights into the European market for bio-based chemicals" [7]. However, limonene production is still low, reaching about 70,000 tons/year globally and 4000 tons/year in European countries [2]. Low limonene availability on the market and the need for extraction and purification steps affect its economic value: its production cost is 8.55 euro/kg, while its commercial price nowadays reaches about 67 euro for 1 L of product [8].

Therefore, innovative strategies are needed for increasing limonene production while decreasing its costs. Indeed, spent OPs obtained after limonene extraction still hold interesting properties that make them suitable materials for further valorization.

In particular, this research work proposes an innovative lab-scale "sequential biorefinery" for a complete valorization of OPs able not only to extract limonene, but also to valorize the by-products of the process by producing volatile fatty acids (VFAs) and activated carbon (AC) (Fig. 1). At first, the solid/liquid (S/L) extraction by *n*-hexane (solvent with a water-octanol partition coefficient very close to the one of limonene) was processed to extract the orange essential oil (OEO) from OPs, rich in limonene. In particular, the operational parameters have been already optimized in a previous work [9], where *n*-hexane, under a temperature of 85 °C and a solvent-OP ratio of 1:2, allowed for reaching an OEO yield (OEOY) of 1.31% with a limonene content up to 90%. Then, the extracted OPs were exploited for both VFA and AC production. VFAs are carboxylic acids adopted as main substrates for the biological production of different products, such as biopolymers, and biofuels [10]. For these reasons, VFA separation from the other organic compounds is crucial to implement the production of innovative biomaterials. Two different batch adsorption tests were conducted to first select the best adsorbent material in terms of VFA separation and, subsequently, evaluate the regeneration of the selected adsorbent and the tolerated number of cycles before its exhaustion. Part of the extracted OPs was also tested under pyrolysis conditions for the production of biochar and further thermally activated with CO_2 to obtain AC, a carbonaceous and highly porous material widely used in many fields of applications (e.g., filtration, adsorption, storage, purification, catalysis) [11].

2 Materials and methods

2.1 OP and inoculum characterization

OPs were collected from the cafeteria of the Department of Biotechnology of the University of Verona, where oranges are squeezed for juice production. Unlike the industrial process in

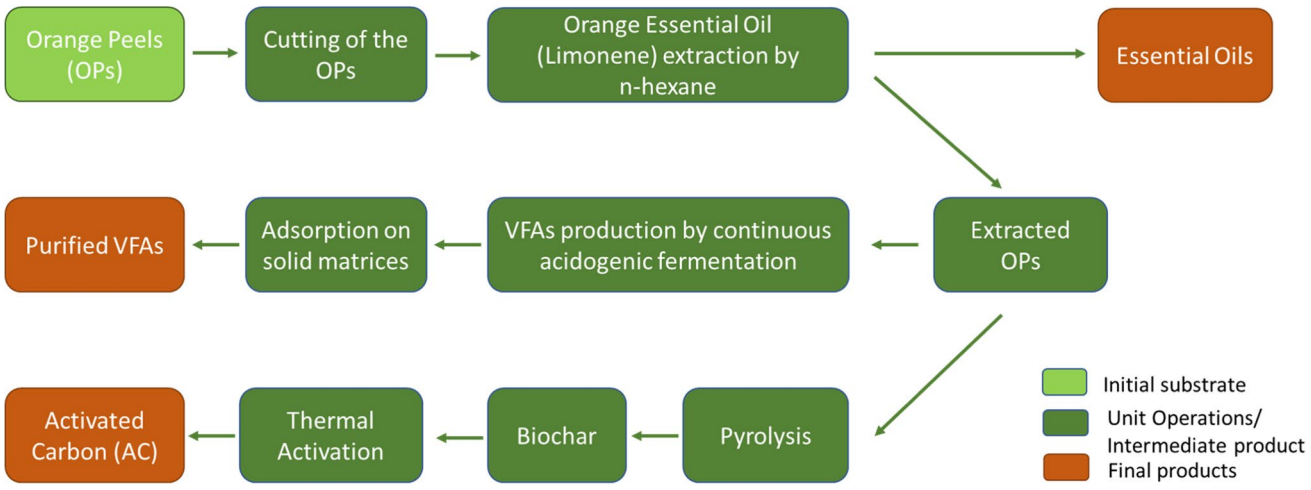

Fig. 1 Main phases of the sequential biorefinery proposed for the valorization of OPs

which juice and essential oils (EOs) are extracted at the same time [3], in this case, EOs are retained in the peels making this type of OPs more appealing for further EO extraction than the industrial ones. After collection, OPs were blended and sieved to consider only particle sizes lower than 2 mm. Then, they were kept in an oven at 60°C for 3 days to evaporate the water content prior to characterization and testing [4]. OP main chemical and physical properties in terms of total solids (TS), total volatile solids (TVS), soluble chemical oxygen demand (sCOD), and pH are summarized in Table 1.

Regarding TS of OP raw, the value measured (37.96%) is higher compared to what is reported in the literature for OPs (17.8–21.3%) [4, 6, 12]. The difference among values may lie in the difference among OP origins since the squeezing in cafeterias might be more effective than the one occurring in industrial processes.

The anaerobic inoculum used for the VFA tests was collected from a biogas plant located in Isola della Scala, (Verona, Italy) treating a mixture of bovine manure, chicken manure, and rice straw and operating at mesophilic conditions (35 °C). OPs after S/L extraction (OP post-ext) and digestate were mixed to reach a TS concentration of 10% w/w, which constituted the feeding of the continuous fermentation tests for VFA production.

2.2 Orange essential oil extraction

At first, OPs were oven-dried at 60 °C until constant weight. The drying temperature was selected to minimize the evaporation of limonene, the boiling temperature of which is 178 °C [13]. Secondly, 50 g of dried OPs was used for the S/L extraction tests in a Soxhlet apparatus (Exacta Optech, Italy), using *n*-hexane as solvent according to the results of authors' previous work [9]. Then, OP sample was placed in a cellulose extraction thimble (WHATMAN Cat. No. 2800-373), plugged with cotton, and located in the Soxhlet extractor. 300 mL of *n*-hexane (Sigma Aldrich) was used to recover the OEO at 85 °C using a solvent-to-OP ratio of 1:2. These operational parameters were retrieved from Battista et al. [9].

The extracts (OEO-solvent mixture) were transferred into a laboratory distillation system to evaporate *n*-hexane until reaching constant weight. The amount of the *n*-hexane recovered from the distillation apparatus was measured to evaluate the solvent recovery yield. The performances of the S/L extraction were assessed in terms of OEO recovered from OPs and expressed as OEO yield (OEOY), calculated according to Eq. (1):

$$\text{OEOY (\%w/w)} = \left(M_{\text{oil}}\right)/\left(M_{\text{OPs}}\right) \bullet 100 \quad (1)$$

where M_{oil} is the mass of the extracted OEO and M_{OPs} is the mass of the dried OPs.

To determine the OEO composition, spectrometry (MS) and flame ionization detector (FID) analyses were carried out by an external laboratory, which conducted an HPLC analysis based on the GC/MS/FID system.

2.3 OP fermentation for VFA production

After limonene solid-liquid extraction, part of the OP post-ext was dried in a chemical hood, until reaching a constant weight, to remove *n*-hexane solvent. Then, it was exploited for VFA production by acidogenic fermentation in a continuous-flow stirred-tank reactor (CSTR), equipped with a Pyrex glass reactor, at a TS concentration of 10% w/w. The CSTR operated at a working volume of 1 L at 200 rpm, under mesophilic temperature (35 °C), with a hydraulic retention time (HRT) of 5 days. In order to reach stable conditions, the duration of the acidogenic fermentation was 3 HRT (15 days). During the start-up of the reactor, corresponding to the first HRT period, the glass vessel was filled with 1 L of the OP post-ext-digestate mixture (the "feeding", see Table 1). Before the beginning of the test, the pH of the feeding was adjusted at neutral condition, which was demonstrated to be the best condition for VFA production [10]. During the first HRT period, the reactor operated in the batch mode and the pH was manually adjusted once a day. From the second HRT period (day 6), 200 mL of feeding, corresponding to a dilution factor of 0.2 day^{-1}, and the reaction medium were fed and discharged, respectively, once a day, until the end of the acidogenic test. The pH was adjusted immediately after the daily feeding of the reactor.

pH, TS, TVS, sCOD, and VFA concentrations of the reaction medium were measured to evaluate the stabilization and the performance of the reactor.

Table 1 Properties of raw OPs, OPs after extraction, inoculum (digestate), and feeding of the continuous VFA production test (nd stays for "not determined")

	OP raw	OP post-ext	Digestate	Feeding
TS (% w/w)	37.96 ± 0.03	95.90 ± 1.09	2.26 ± 0.01	9.92 ± 1.44
TVS/TS (%)	96.41 ± 0.01	93.01 ± 0.27	57.28 ± 0.03	96.57 ± 0.69
sCOD (g/L)	nd	nd	30.21 ± 3.59	52.96 ± 2.66
pH	nd	nd	8.83 ± 0.02	4.29 ± 0.02

The performance of the acidogenic fermentation was evaluated considering the specific VFA yield, determined by the ratio between the daily VFA production rate (gVFAs/day) and the grams of TS fed per day (gTS fed/day), as follows (Eq. 2):

$$\text{Yield}_{\text{totVFAs}} = \frac{\text{gVFAs/day}}{\text{gTS fed/day}} \quad (2)$$

2.4 Adsorption tests for VFA recovery

In order to recover the VFAs from the fermentation broth, two different batch adsorption tests were conducted. A first experimental campaign was performed using four different solid matrices in 15-mL falcons: (a) powdered activated carbon (PAC) 7440-44-0, (b) Dowex M4195, (c) Lewatit VP OC 1065 (primary amine), (d) Amberlyst A-21 (tertiary amine) (see details in Section 2.4.1). The second set of adsorption tests was conducted in a glass column filled with the solid matrix selected from the first experimental campaign to evaluate the regeneration of the matrix and, consequently, the maximal number of cycles for its utilization (see details in Section 2.4.2).

The daily output (reaction medium) from the acidogenic fermentation was filtered at 0.2 µm using a vacuum pump and its VFA content was measured before and after the adsorption tests.

The adsorption tests (first and second round) were carried out in triplicate at a temperature of 30 °C, consistent with the mesophilic condition of the acidogenic fermentation of VFAs [14].

2.4.1 First round of adsorption tests

The chemical and physical properties of the different adsorbents used are summarized in Table 2.

The batch tests were performed in 15-mL falcons with a working volume of 10 mL using 0.5 g (50 g adsorbent/L) of solid matrices, replicating the procedures of some previous works [15–17]. The samples were shacked for 3 h on a laboratory shaker at 150 rpm to favor the VFA diffusion in the falcons and their adsorption on the solid matrices.

The tests were evaluated in terms of VFA and sCOD adsorption yields (Eq. 3 and 4) and selectivity of VFA adsorption (Eq. 5), defined as follows:

$$\text{VFA Adsorption yield (\%)} = Y\ \text{VFA ads} = \frac{C_0 - C_e}{C_0} \bullet 100 \quad (3)$$

$$\text{sCOD Adsorption yield (\%)} = Y\ \text{sCOD ads} = \frac{sCOD0 - sCODe}{sCOD0} \bullet 100 \quad (4)$$

$$S_{\text{VFA}}\ (\%) = \frac{Q\ \text{VFAs ads}}{Q\ \text{sCOD ads}} \bullet 100 \quad (5)$$

where C_0 is the total VFA concentration of the reaction medium after the acidogenic fermentation (mg/L); C_e is the equilibrium concentration of the total VFAs after adsorption (mg/L); sCOD0 is the sCOD concentration of the reaction medium after acidogenic fermentation (mg/L); sCODe is the sCOD equilibrium concentration after adsorption; $Q_{\text{VFAs ads}}$ is the VFA amount adsorbed by the solid matrix (mg), while $Q_{\text{sCOD ads}}$ is the sCOD amount adsorbed by the solid matrix (mg). Thus, S_{VFA} parameter indicates the ability of the solid matrix to adsorb preferentially the VFAs than the other organic compounds after the acidogenic fermentation.

2.4.2 Second round of adsorption tests

Since PAC proved to be the optimal matrix for the separation of the VFAs from the other organic compounds, the second round of adsorption tests was performed only on PAC using a chromatographic glass column as an adsorption column, having a height of 50 cm and a diameter of 2.5 cm. To avoid PAC packing and to increase the available surface area, the column was firstly filled with glass wool, while the bottom was covered with a glass wool/cotton mixture to allow for a slow discharge of the reaction medium entering from the top of the column. In this way, a residence time of about 1 h was assured for the reaction medium in the column. Then, the column was filled with 10 g of PAC. The second round of adsorption tests was conducted by introducing 20 mL of reaction medium, keeping constant the ratio between the volume of the reaction medium and the mass of the solid matrix, already tested in the previous experiments.

Table 2 Properties of adsorbents used: PAC 7440-44-0, DOWEX M4195, Lewatit VP OC 1065, Amberlyst A-21 (*ns*, not specified in the technical sheet)

	PAC 7440-44-0	DOWEX M4195	Lewatit VP OC 1065	Amberlyst A-21
Chemical composition	Carbon	Styrene-divinylbenzene tertiary amine (bis-picolylamine)	Styrene-divinylbenzene primary amine (benzyl amine)	Styrene-divinylbenzene tertiary amine (ns)
Particle size (mm)	0.001–0.150	0.29–0.84	0.47–0.57	0.49–0.69
Approx. pore volume (cm^3/g)	0.65	ns	0.27	0.10
Approx. surface area (m^2/g)	> 800	ns	50	35

At the end of each adsorption cycle, the PAC was regenerated using 10 mL of an ethanol solution concentrated in sodium hydroxide (1M), which usually leads to high-regeneration performances [17]. Then, the reaction medium was reintroduced in the regenerated column to evaluate the number of cycles of utilization of PAC before its performance decay.

2.5 Biochar and activated carbon production

Before analysis and testing, part of OP post-ext was stabilized in oven at 45 °C for 48 h and then crushed using a mortar.

Biochar (OP biochar) was produced through slow pyrolysis in a simultaneous thermal analyzer (STA 449 F3 Jupiter, Netzsch). 750 mg of stabilized sample was placed in a 5 mL alumina crucible and then heated up to 105 °C at 20 °C/min. Nitrogen was used as protective and purge gas (20 mL/min). The temperature was kept constant for 1 h to remove the residual moisture. Subsequently, temperature was raised to 550 °C at 10 °C/min and kept constant for 1 h.

The same thermogravimetric analyzer was used to physically activate the obtained biochar using CO_2 as activating agent (see Fig. 2). After pyrolysis, the temperature was raised to 800 °C at 10 °C/min in inert atmosphere. Once the activation temperature was reached, the purge gas was switched to a mixture of CO_2 and N_2 (CO_2:N_2=1:2), and the temperature was kept constant for 1 h. Finally, the system was left to cool down under a nitrogen flow and activated biochar (OP AC) was collected. Activation conditions were selected to ensure the best trade-off between burn-off and porosity development [18].

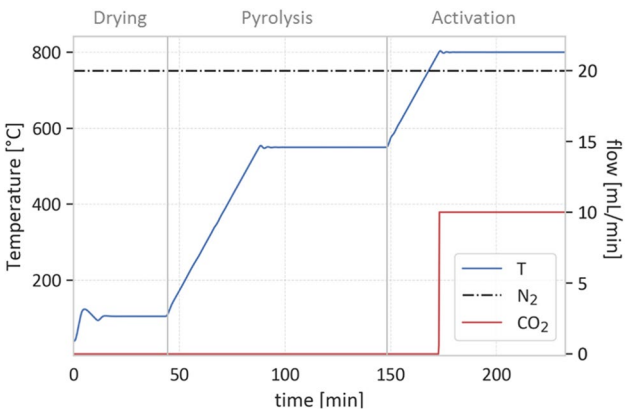

Fig. 2 Temperature program and gas fluxes used during the drying, pyrolysis, and activation stages

2.6 Analytical methods

The pH of the samples and the pH during the different analyses were measured by a benchtop pH meter (Mettler Toledo, USA). TS, TVS, and sCOD were determined according to the Standard Methods [19]. In order to determine single and total VFA concentration, distilled water was used to dilute the samples in a substrates-water ratio of 1:100 and then filtered at 0.20 µm. Then, the concentrations of the VFAs were measured by ionic chromatography (Dionex ICS-1100 with AS23 column, Thermo Fisher Scientific, USA).

Pyrolysis of OP post-ext was characterized by coupling thermogravimetric analysis with FT-IR for evolved gas analysis. In each test, about 10 mg of the sample was analyzed in the simultaneous thermal analyzer to obtain mass loss profiles during heating. To monitor the effect of temperature on gas evolution, a FT-IR spectrometer (Tensor 27, Bruker) was connected to the thermogravimetric analyzer through a transfer line kept at 200 °C. The system was equipped with a liquid nitrogen-cooled MCT (mercury-cadmium-telluride) detector; a resolution of 4 cm^{-1} every 15 s, with 32 scans of every sample measurement in the range of spectrum between 4000 and 628 cm^{-1}, was selected to record the IR spectra. A baseline correction was applied to all spectra using a concave rubber band correction algorithm with 10 iterations computed over 64 points, including CO_2 band, and the offset method was used to normalize the results. Noise was reduced thanks to a Savitzky-Golay filter, and finally, processed data were plotted for the analysis of the results [20].

Proximate analysis was performed by a simultaneous thermal analyzer (Jupiter STA 449 F3, Netzsch) to determine the moisture, volatile matter, fixed carbon, and ash content of raw orange peel (OP raw), OP post-ext, OP biochar, and OP AC. Firstly, the moisture content was assessed by letting the sample at 100 °C for 40 min in N_2 atmosphere, then the sample was heated up to 900 °C in N_2 for about 5 min to determine the volatile matter content. Subsequently, fixed carbon content was evaluated decreasing the temperature from 900 to 400 °C. Finally, the purge gas was switched to chromatographic air and the temperature increased to 550 °C for 40 min promoting the complete combustion of the remaining fixed carbon. The residual weight after combustion was recorded and identified as the ash content.

Carbon, hydrogen, nitrogen, and sulfur content in OP raw, OP post-ext, OP biochar, and OP AC, were measured by a Vario MACRO Cube (Elementar) elemental analyzer. Oxygen was calculated by difference.

Higher heating value (HHV) was assessed using an isoperibolic calorimeter (IKA C200).

Specific surface area, pore volume, and pore size of OP biochar and OP AC were measured using a 3Flex Surface Characterization Analyzer (Micromeritics Co.) operating with N_2 at −196 °C. Before analysis, samples were degassed

ex situ at 250 °C overnight and then, vacuum degassed in situ at 250 °C for 3 h. The specific surface area was determined by the Brunauer-Emmett-Teller (BET) method [21], while the pore size distribution was obtained by Barret-Joyner-Halenda (BJH) desorption analysis [22].

3 Results and discussions

3.1 Orange essential oil extraction

OEO extraction was carried out using *n*-hexane under the operational parameters previously reported. *n*-Hexane has a polar index very close to zero, which made compatible with revealing limonene, a no-polar molecule. Moreover, *n*-hexane presents a water-octanol partition coefficient (K_{ow}) of 3.6, which reveals its lipophilic nature as the one of limonene, with $K_{ow} = 4.2$. For this reason, *n*-hexane led to a OEOY in the range of 0.80–1.20% w/w, one of the highest OEOY currently reported in the scientific literature for solvent extraction. Indeed, to the best of the authors' knowledge, only Ozturk et al. [23], who tested different solvents to extract limonene from OPs provided by a local juice bar, achieved a slightly higher OEO extraction yield of about 1.50% w/w using cyclopentyl methyl ether as solvent. It is important to underline that other extraction techniques, such as freeze drying, allowed for reaching higher OEOY of about 7% v/w corresponding to about 5.9–6.0% w/w. In this case, the limonene content in the oil (extracted from OPs deriving from an orange juice production plant) was about 80% [12].

Regarding the composition of OEO extracted through *n*-hexane in this work, D-limonene was the main constituent counting for 94% w/w, followed by β myrcene with 3% w/w. This result well complies with the results of previous works [9, 24, 25].

3.2 OP fermentation for VFA production

After limonene extraction, part of OP post-ext was fed in a CSTR for acidogenic fermentation at the operational conditions previously described. Figure 3 summarizes the evolution of the main parameters during the acidogenic fermentation.

The TS and TVS/TS trends are shown in Fig. 3A. As above, the TS of the reactor feeding was 9.92 ± 1.44 %. During the start-up period, the TS and the TVS/TS remained constant at around 9% w/w and 93%, respectively. Then, they decreased reaching the stable value of about 7.5% w/w and 70% in the second half of the acidogenic fermentation test. A similar trend was observed for the sCOD, which was constant during the start-up of the reactor (62–65 g/L) and decreased to 45 g/L until the eighth day of fermentation (Fig. 3B). The higher values registered for the parameters in the initial phase than in the final phase are due to the lag phase of the microorganisms.

On the contrary, the VFA concentration was very low during the first hours of fermentation and started to increase only during the second day of testing (Fig. 3B) as a consequence of the conversion of the sugars contained in the OPs. In fact, OPs are rich in soluble sugars (glucose, fructose), which were promptly and easily hydrolyzed into VFAs by the microorganisms. Then, with the beginning of the hydrolyzation and the conversion of hemicellulose and cellulose, the VFA concentration reached a stable level of 7.5 g/L, corresponding to a VFA production yield of 42.8%, referred to the TS content of the feeding. This value is higher than the

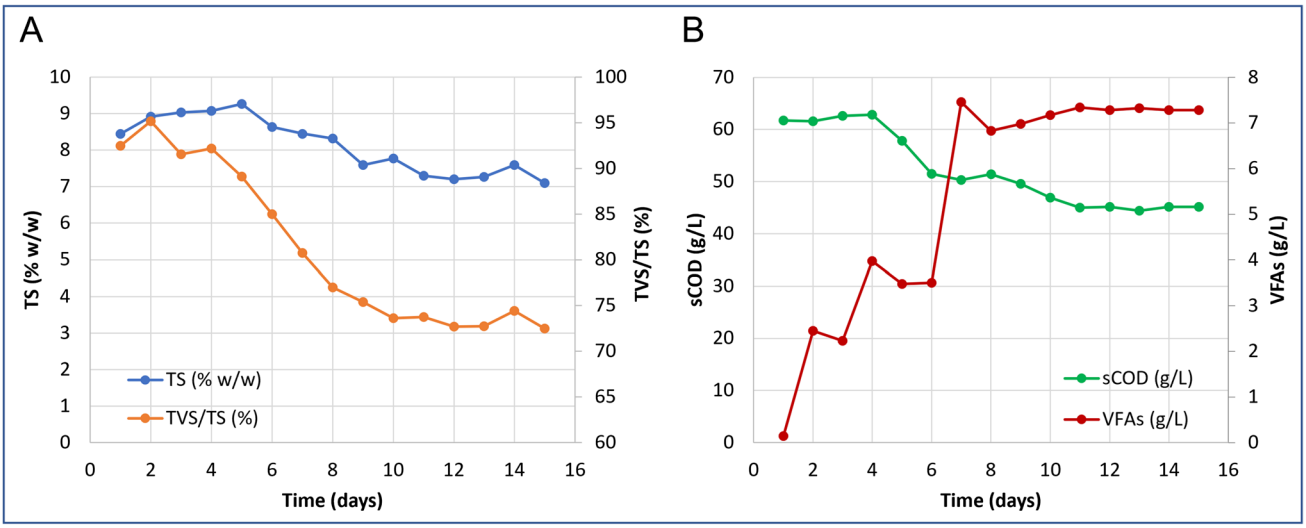

Fig. 3 Evolution of TS and TVS/TS (**A**), sCOD and VFAs (**B**) during acidogenic fermentation

best VFA production yield of 34% achieved by Battista et al. [9], who conducted the acidogenic fermentation of OPs in a reactor operating at 15% w/w in batch configuration with daily manual agitation. Probably, the higher values obtained in the present work are related to the continuous agitation of the reactor at 200 rpm, which helped the physical desegregation of the OPs and improved the heat and mass transfer. As far as the composition is concerned, VFAs consisted of 75% w/w acetic acid and 25% w/w formic acid. Acetic and formic acids are the main VFAs coming from short HRT acidogenic fermentation, as the formation of longer VFAs usually requires longer time [26].

One by-product of acidogenic fermentation is represented by biogas. At steady-state conditions, the daily biogas production was around 1.2–1.5 NL/L, composed of 90% CO_2 and 10% H_2. Methane was not detected as the continuous test was set up at an HRT of 3 days, too short to allow the starting of the methanogenic phase of the anaerobic digestion. Consequently, at this condition, the methanogenic microorganisms were washed out from the reactor [27]. The biogas production justifies the decrease of the TS, TVS/TS, and sCOD concentrations between the inlet and outlet streams [28].

3.3 Adsorption tests for the VFA recovery

3.3.1 First round of adsorption tests

A first round of batch adsorption tests was performed to select the best solid matrix in terms of VFA separation from the other organic compounds present in the reaction medium.

Figure 4 summarizes the main results of the adsorption tests.

Low VFA and sCOD adsorption yields were measured (< 30%) due to the saturation of the solid matrices meaning that most of the organic compounds remained in the reaction medium, without being adsorbed. However, saturation had also a positive impact as it allowed us to observe the competition in adsorption among the different organic molecules. In this way, it was possible to determine which compounds are preferentially adsorbed by each specific solid matrix [17]. The VFA adsorption yields were around 20% for all the matrices, except for Amberlyst which achieved almost 30%. The adsorption yield of all the soluble organic matter, expressed in terms of sCOD, was about 25–30% for the ionic exchange resins (Dowex, Amberlyst, and Lewatit) but closer to 50% for PAC. These first results are consistent with the ones obtained in the authors' previous work, where adsorption tests were conducted on synthetic VFAs [17]. Amberlyst and Lewatit had higher VFA adsorption performances than PAC due to the higher chemical affinity of VFAs to Amberlyst and Lewatit than PAC [17].

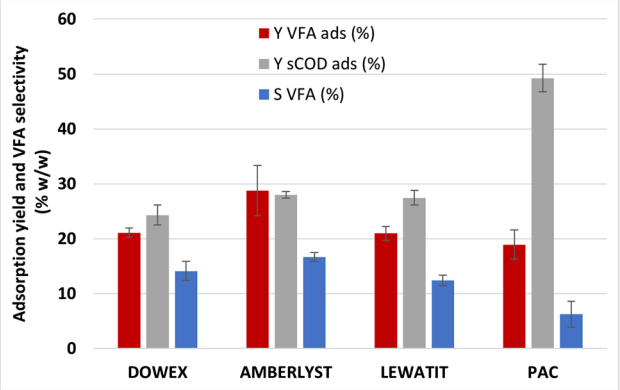

Fig. 4 Adsorption yields and VFA selectivity (%w/w) for the different solid matrices (*Y ads*, adsorption yield; *S*, selectivity)

Considering the ability to separate VFAs from the reaction medium, all the ionic exchange resins seemed to adsorb the VFAs and the other organic matter in the same way, as demonstrated by the similar values of VFA and sCOD adsorption yields (Fig. 4). It means that these resins are not suitable for the VFA separation as they left almost unaltered the ratio between the VFAs and sCOD of the reaction medium. The VFA selectivity parameter was low and around 10–15% for the three resins.

PAC behavior was different: the VFA adsorption yield was the lowest among all the solid matrices (19%), while the sCOD adsorption yield (around 50%) was the highest one, demonstrating the good tendency of PAC to adsorb no-VFA compounds. Consequently, the S_{VFA} measured for PAC was very low, about 6%. Since PAC was the only solid matrix showing an adsorption discrimination between VFA and no-VFA compounds, it could be exploited to obtain a purified VFA solution. In fact, when PAC was used for the VFA separation from the reaction medium, the VFAs/sCOD ratio increased from 16 to almost 30%, while remained almost constant (16–18%) when Dowex, Amberlyst, and Lewatit were applied. To the best of the authors' knowledge, VFA recovery from real fermentates has been little investigated in previous works, and calculation of VFA selectivity has never been reported, thus representing one of the most innovative aspects of this work.

3.3.2 Second round of adsorption tests

After selecting PAC as the best adsorbent for the VFA separation from the reaction medium, a second round of batch adsorption tests was performed in a laboratory glass column to evaluate the regeneration of PAC and, consequently, the maximal number of cycles for its utilization. For this scope, 10 mL of an ethanol solution in sodium hydroxide (1M) was adopted as eluent. Table 3 reports the adsorption

Table 3 Adsorption and desorption performances at different cycles on PAC

N. of cycles on PAC	Y VFA Ads (%)	Y sCOD Ads (%)	Y sCOD Des (%)	VFA/sCOD ratio (%)
1	20.55 ± 0.14	55.69 ± 3.14	44.16 ± 1.65	28.23 ± 0.90
2	21.33 ± 1.54	40.87 ± 1.07	31.92 ± 0.90	37.76 ± 1.28
3	5.28± 0.30	11.43 ± 0.82	10.09 ± 0.43	40.23 ±0.75

and desorption performances of 20 mL of reaction medium along three cycles on PAC.

The first cycle showed very similar performances to the ones obtained in the previous experimental adsorption tests: the VFA and sCOD adsorption yields were 20 and 55%, respectively, and the final VFA/sCOD ratio was 28%. The sCOD desorption yield was 44%, which means that the major part of the organic matter remained adsorbed on PAC. The output reaction medium from the first adsorption cycle was fed into the column again. This second cycle on PAC gave almost the same VFA adsorption yield (about 21%), but a lower sCOD adsorption one (about 40%). The VFA/sCOD ratio increased to almost 38%. Desorption regeneration performance was lower, passing from 44% in the first cycle to 32% in the second one, revealing the beginning of the PAC saturation. Finally, the third cycle was characterized by very low yields and a VFA/sCOD ratio, which slightly increased to 40%.

This second round of adsorption tests demonstrated that PAC has not a good tendency to desorb some organic molecules, preventing a longer usage of the same PAC amount. Probably, a higher volume of eluent could help increase the number of cycles.

3.4 OP pyrolysis and derived biochar activation

3.4.1 Evolved gas analysis

Thermal degradation of OP after extraction in inert atmosphere occurs in three main steps (see Fig. 5). Indeed, derivative thermogravimetric (DTG) analysis shows three main peaks at 205, 220, and 340 °C corresponding to the degradation of water-soluble components, hemicellulose, and cellulose, respectively [29]. The continuous mass loss occurring at temperatures higher than 400 °C corresponds to the degradation of lignin and charring process[30].

The identified FT-IR absorption peaks were attributed to characteristic bond vibrations in functional groups of molecules (see Fig. 6) [31, 32]. The O-H stretching vibration at 4000–3500 cm^{-1} was attributed to H_2O as consequence of dehydration reactions. The large absorption peak at 3000–2600 cm^{-1} was identified as -CH bond stretching vibration in alkanes and alkyl functional groups (e.g., CH_4, $-CH_3$, $-CH_2$), while the characteristic peak at 2400–2250 cm^{-1} was due to C=O double bond vibrations of CO_2. Peaks

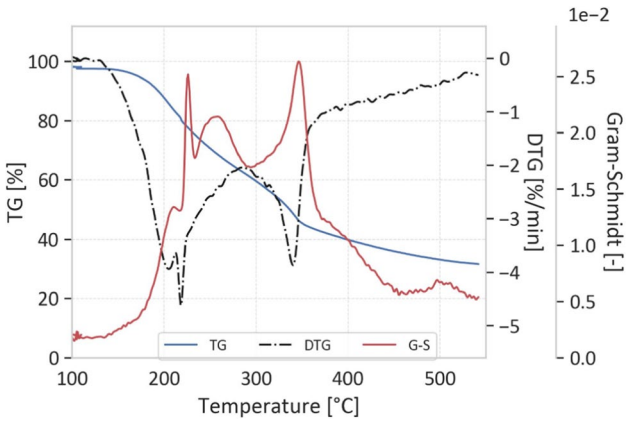

Fig. 5 TG, DTG, and Gram-Schmidt curves obtained for OP post-ext

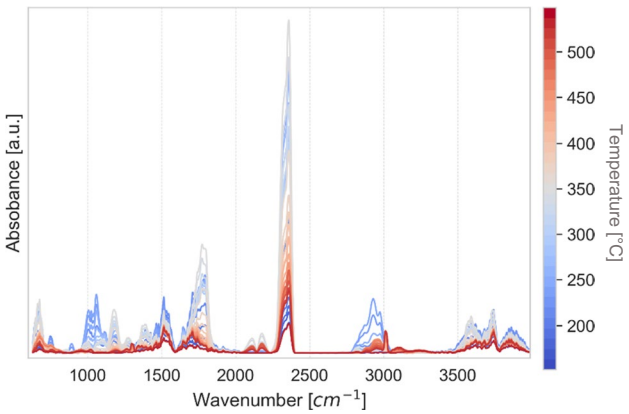

Fig. 6 Evolved gas analysis results

at 2250–2000 cm^{-1} were attributed to CO formation. Carboxylic acids, ketones, and aldehydes vibrations are responsible for the 1800–1600 cm^{-1} absorption region. To conclude, the peaks in the region from 1250 to around 1000 cm^{-1} were likely due to C-O stretching vibrations of other organic molecules (e.g., alcohols, phenols, ethers).

The amount of water and CH_4 decreased with temperature while the amount of CO_2, carboxylic acids, and ketones increased until reaching 350 °C and then decreased with increasing temperatures. The same temperature-dependent evolution trend was seen for aromatics and alkanes. So, it can be concluded that hemicellulose and cellulose degradation are likely to be the main ones responsible for the release of the

volatile compounds. The release of CO_2 at medium temperatures is generally related to the degradation of the lateral chains in the lignin polymer and the thermolabile functional groups, such as aliphatic hydroxyl, carboxyl, and carbonyl groups, while the CH_4 releases were related to the conversion of alkyl chains and the removal of methoxyl substituents in the substrate [33].

3.4.2 Proximate and ultimate analysis

Proximate analysis results (Table 4) show that extraction did not affect volatile matter, fixed carbon, and ash content of OPs. As expected, volatile matter decreases from 71.94 to 12.72% after pyrolysis and to 8.37% after activation, while fixed carbon content and ash content increased from 21.93 to 75.22 %, and from 3.26 to 13.93%, respectively. Indeed, during pyrolysis large molecules of biomass particles decompose into condensable gases and non-condensable gases, which leave the solid matrix decreasing the volatile matter, and into char (OP biochar in this case), the solid residue with a high carbon content and thus, an increased fixed carbon content compared to the precursor [29]. Moreover, the harsher conditions of physical activation compared to pyrolysis accentuate these effects.

As shown in Table 5, extraction did not affect elemental composition and HHV of orange peel either, except for the sulfur content, which decreases from 0.24 to 0.13%. Due to biomass carbonization occurring during pyrolysis, C and N contents of biochar were higher than its precursor, while H and O contents decreased. Carbonization also increases the HHV from 16.51 MJ/kg for OP after extraction to 29.39 MJ/kg for OP biochar. Activation at 800 °C in a CO_2/N_2 atmosphere led to a further increase in the C and N content to 86.10 and 1.86%, respectively, and a decrease in the H content to 0.65%.

3.4.3 Physisorption analysis

Table 6 shows the results of the physisorption analysis obtained for OP biochar and OP AC, where also results retrieved from the literature on similar materials are reported for comparison. Physical activation of OP biochar increased its surface area by almost ten times, from 40 to 326 m^2/g, proving the effectiveness of the treatment. Although pore volume was not affected, the average pore size drastically decreased from 44.99 to 9.44 nm, always in the range of mesopores (2 ÷ 50 nm).

Results well comply with previous studies on raw OP (see Table 6). However, harsher carbonization and activation conditions (i.e., chemical activation and microwave pyrolysis) could lead to a better porosity development (i.e., S_{BET} = 1015 m^2/g, V_{pore} = 0.5 cm^3/g, d_{pore} = 1.5 nm [36]) and to the production of materials more similar to commercial AC.

According to the BDDT (Brunauer-Deming-Deming-Teller) classification [37], isotherm for OP biochar can be classified as type III isotherm, related to the weak gas-solid interactions typical of macro-porous materials. On the other hand, isotherm for OP AC can be classified as type IV isotherm, characteristic of mesoporous structures. Moreover, it displays a type III hysteresis loop at relative pressure higher than 0.4, indicative of the presence of slit pores. It should be noticed that both isotherms take on a

Table 4 Proximate analysis results

	Moisture %	Volatile Matter %	Fixed Carbon %	Ash %
OP raw	4.12 ± 0.67	71.52 ± 0.33	20.83 ± 0.11	3.53 ± 0.89
OP post-ext	2.87 ± 0.59	71.94 ± 0.175	21.93 ± 0.08	3.26 ± 0.34
OP biochar	1.89 ± 0.25	12.72 ± 0.22	74.22 ± 0.16	11.17 ± 0.63
OP AC	2.49 ± 0.18	8.37 ± 0.04	75.22 ± 1.17	13.93 ± 1.31

Table 5 Ultimate analysis results and higher heating values (*HHV*)

	C $\%wt_{dry}$	H $\%wt_{dry}$	N $\%wt_{dry}$	S $\%wt_{dry}$	O* $\%wt_{dry}$	HHV MJ/kg
OP raw	43.14 ± 0.70	6.16 ± 0.10	0.62 ± 0.07	0.24 ± 0.06	46.29	16.83 ± 0.09
OP post-ext	43.94 ± 0.11	6.36 ± 0.05	0.72 ± 0.03	0.13 ± 0.01	45.59	16.51 ± 0.04
OP biochar	82.88 ± 0.50	2.30 ± 0.04	1.54 ± 0.09	0.12 ± 0.01	1.99	29.39 ± 0.36
OP AC	86.10 ± 1.35	0.65 ± 0.03	1.86 ± 0.03	0.13 ± 0.01	nd	27.19 ± 0.14

*Oxygen calculated by difference

Table 6 Physisorption analysis results and data from the literature

	Activating agent	Pyrolysis/activation temperature	S_{BET}	Pore volume	Pore size	Ref.
		°C	m^2/g	cm^3/g	nm	
OP biochar	-	550	40 ± 3	0.37 ± 0.01	44.99 ± 0.33	This study
OP AC	CO_2	800	326 ± 2	0.31 ± 0.00	9.44 ± 0.02	This study
OP biochar	-	500	105	0.04	4	[34]
OP AC	CO_2	500–1200	225–248	-	7–14	[35]
OP AC	KOH	Microwave activation	1015	0.5	1.5	[36]
Commercial AC	-	-	650–1200	0.7–1.3	1.8–4	[36]

hyperbolic shape close to $p/p^\circ = 1$, associated with the presence of macropores.

4 Conclusions

A biorefinery approach was tested at the laboratory scale for the valorization of OPs following the waste hierarchy promoted by the EU. In particular, at first, limonene—a high added value compound—was extracted. Then, the spent material was further valorized for the production of VFAs and AC. Solid-liquid extraction of OPs for limonene recovery was performed in a Soxhlet apparatus using *n*-hexane as solvent under a OP:solvent of 1:2. In this way, a limonene recovery of about 1.20% w/w was obtained. After extraction, part of OPs was used for the VFA production in continuous mode under an HRT of 5 days and an inlet TS concentration of about 10% w/w, obtaining a VFA yield of 43% (g_{VFAs}/g_{TS}). The purification of the VFAs was conducted by adsorption on the same PAC as solid matrix, able to adsorb essentially no-VFA compounds. Three cycles of the fermentation broth on PAC increased the VFA/sCOD ratio from 16 to 40% w/w.

The remaining part of OP post-ext was converted into biochar through slow pyrolysis at 550 °C for 1 h using a thermogravimetric analyzer coupled with a FT-IR spectrometer, which allowed the thorough characterization of the process. Subsequently, in the same analyzer, the biochar obtained was physically activated with CO_2 (CO_2:N_2=1:2) at 880 °C for 1 h to produce AC. According to the characterization results, the first extraction step did not appreciably affect OP properties, while pyrolysis increased the carbon content (from 43 to 83%) and the heating value (from 17 to 29 MJ/kg) of the material. Physical activation of OP biochar increased it surface area of almost ten times, from 40 to 326 m^2/g, proving the effectiveness of the treatment.

These promising results suggest that the implementation and scale-up of a biorefinery approach similar to the one here proposed could have beneficial impacts on the orange fruit value chain, leading to the production of valuable and environmentally friendly compounds and materials, and concurrently to the reduction of waste and the preservation of resources.

Data availability Not applicable.

Author contributions FR: Data curation; formal analysis; investigation; writing—original draft. VB: Conceptualization; data curation; formal analysis; investigation; methodology; validation; visualization; writing—original draft. FP: Conceptualization; methodology; supervision; validation; writing—review and editing. MB: Conceptualization; resources; funding acquisition; supervision; writing—review and editing. DB: Supervision; funding acquisition. FB: Conceptualization; writing—original draft; writing—review and editing; supervision.

Funding Open access funding provided by Libera Università di Bolzano within the CRUI-CARE Agreement.

Declarations

Ethics approval Not applicable.

Competing interests The authors declare no competing interests.

References

1. European Commission (2018) Directive (EU) 2018/851 of the European Parliament and of the Council of 30 May 2018 amending Directive 2008/98/EC on waste (Text with EEA relevance). In: Off J Eur Union, pp 109–140
2. Negro V, Mancini G, Ruggeri B, Fino D (2016) Citrus waste as feedstock for bio-based products recovery: review on limonene case study and energy valorization. Bioresour Technol 214:806–815. https://doi.org/10.1016/j.biortech.2016.05.006

3. Zema DA, Calabrò PS, Folino A et al (2018) Valorisation of citrus processing waste: a review. Waste Manag 80:252–273. https://doi.org/10.1016/J.WASMAN.2018.09.024
4. Fazzino F, Mauriello F, Paone E et al (2021) Integral valorization of orange peel waste through optimized ensiling: lactic acid and bioethanol production. Chemosphere 271:129602. https://doi.org/10.1016/J.CHEMOSPHERE.2021.129602
5. Tovar AK, Godínez LA, Espejel F et al (2019) Optimization of the integral valorization process for orange peel waste using a design of experiments approach: production of high-quality pectin and activated carbon. Waste Manag 85:202–213. https://doi.org/10.1016/J.WASMAN.2018.12.029
6. Calabrò PS, Fazzino F, Sidari R, Zema DA (2020) Optimization of orange peel waste ensiling for sustainable anaerobic digestion. Renew Energy 154:849–862. https://doi.org/10.1016/J.RENENE.2020.03.047
7. Spekreijse J, Lammens T, Parisi C, et al (2019) Insights into the European market for bio-based chemicals
8. Sigma Aldrich (2021) www.sigmaaldrich.com
9. Battista F, Remelli G, Zanzoni S, Bolzonella D (2020) Valorization of residual orange peels: limonene recovery, volatile fatty acids, and biogas production. ACS Sustain Chem Eng 8:6834–6843. https://doi.org/10.1021/acssuschemeng.0c01735
10. Strazzera G, Battista F, Tonanzi B et al (2021) Optimization of short chain volatile fatty acids production from household food waste for biorefinery applications. Environ Technol Innov 23:101562. https://doi.org/10.1016/j.eti.2021.101562
11. Benedetti V, Patuzzi F, Baratieri M (2018) Characterization of char from biomass gasification and its similarities with activated carbon in adsorption applications. Appl Energy 227:92–99. https://doi.org/10.1016/j.apenergy.2017.08.076
12. Wikandari R, Nguyen H, Millati R et al (2015) Improvement of biogas production from orange peel waste by leaching of limonene. Biomed Res Int 2015. https://doi.org/10.1155/2015/494182
13. IPCS Inchem, https://inchem.org/documents/icsc/icsc/eics0918.htm
14. Freitas AF, Mendes MF, Coelho GLV (2007) Thermodynamic study of fatty acids adsorption on different adsorbents. J Chem Thermodyn 39:1027–1037. https://doi.org/10.1016/j.jct.2006.12.016
15. Eregowda T, Rene ER, Rintala J, Lens PNL (2020) Volatile fatty acid adsorption on anion exchange resins: kinetics and selective recovery of acetic acid. Sep Sci Technol 55:1449–1461. https://doi.org/10.1080/01496395.2019.1600553
16. Yousuf A, Bonk F, Bastidas-Oyanedel JR, Schmidt JE (2016) Recovery of carboxylic acids produced during dark fermentation of food waste by adsorption on Amberlite IRA-67 and activated carbon. Bioresour Technol 217:137–140. https://doi.org/10.1016/j.biortech.2016.02.035
17. Rizzioli F, Battista F, Bolzonella D, Frison N (2021) Volatile fatty acid recovery from anaerobic fermentate: focusing on adsorption and desorption performances. Ind Eng Chem Res 60:13701–13709. https://doi.org/10.1021/acs.iecr.1c03280
18. Kilpimaa S, Runtti H, Kangas T et al (2015) Physical activation of carbon residue from biomass gasification: novel sorbent for the removal of phosphates and nitrates from aqueous solution. J Ind Eng Chem 21:1354–1364. https://doi.org/10.1016/j.jiec.2014.06.006
19. APHA (1998) Standard methods for examination of water and wastewater, 20th edn. American Public Health Association
20. Paini J, Benedetti V, Ferrentino G et al (2021) Thermochemical conversion of apple seeds before and after supercritical CO2 extraction: an assessment through evolved gas analysis. Biomass Convers Biorefinery 11:473–488. https://doi.org/10.1007/s13399-020-00858-z
21. Brunauer S, Emmett PH, Teller E (1938) Adsorption of gases in multimolecular layers. J Am Chem Soc 60:309–319. https://doi.org/10.1021/ja01269a023
22. Barrett EP, Joyner LG, Halenda PP (1951) The determination of pore volume and area distributions in porous substances. I. Computations from nitrogen isotherms. J Am Chem Soc 73:373–380. https://doi.org/10.1021/ja01145a126
23. Ozturk B, Winterburn J, Gonzalez-Miquel M (2019) Orange peel waste valorisation through limonene extraction using bio-based solvents. Biochem Eng J 151:107298. https://doi.org/10.1016/j.bej.2019.107298
24. Farahmandfar R, Tirgarian B, Dehghan B, Nemati A (2020) Changes in chemical composition and biological activity of essential oil from Thomson navel orange (Citrus sinensis L. Osbeck) peel under freezing, convective, vacuum, and microwave drying methods. Food Sci Nutr 8:124–138. https://doi.org/10.1002/fsn3.1279
25. Ortiz-Sanchez M, Solarte-Toro JC, Orrego-Alzate CE et al (2021) Integral use of orange peel waste through the biorefinery concept: an experimental, technical, energy, and economic assessment. Biomass Convers Biorefinery 11:645–659. https://doi.org/10.1007/s13399-020-00627-y
26. Possente S, Bertasini D, Rizzioli F et al (2022) Volatile fatty acids production from waste rich in carbohydrates: Optimization of dark fermentation of pasta by-products. Biochem Eng J 189:108710. https://doi.org/10.1016/J.BEJ.2022.108710
27. Bolzonella D, Battista F, Cavinato C et al (2018) Recent developments in biohythane production from household food wastes: a review. Bioresour Technol 257:311–319. https://doi.org/10.1016/J.BIORTECH.2018.02.092
28. Angelidaki I, Alves M, Bolzonella D et al (2009) Defining the biomethane potential (BMP) of solid organic wastes and energy crops: a proposed protocol for batch assays. Water Sci Technol 59:927–934. https://doi.org/10.2166/wst.2009.040
29. Basu P (2010) Biomass Gasification and Pyrolysis. Elsevier Inc.
30. Izydorczyk G, Skrzypczak D, Kocek D et al (2020) Valorization of bio-based post-extraction residues of goldenrod and alfalfa as energy pellets. Energy 194. https://doi.org/10.1016/j.energy.2020.116898
31. Ong HC, Chen WH, Singh Y et al (2020) A state-of-the-art review on thermochemical conversion of biomass for biofuel production: a TG-FTIR approach. Energy Convers Manag 209:112634. https://doi.org/10.1016/j.enconman.2020.112634
32. Wu X, Ba Y, Wang X et al (2018) Evolved gas analysis and slow pyrolysis mechanism of bamboo by thermogravimetric analysis, Fourier transform infrared spectroscopy and gas chromatography-mass spectrometry. Bioresour Technol 266:407–412. https://doi.org/10.1016/j.biortech.2018.07.005
33. Song F, Li T, Zhang J et al (2019) Novel insights into the kinetics, evolved gases, and mechanisms for biomass (Sugar Cane Residue) Pyrolysis. Environ Sci Technol 53:13495–13505. https://doi.org/10.1021/acs.est.9b04595
34. Lam SS, Liew RK, Cheng CK, Rasit N, Ooi CK, Ma NL, Ng JH, Lam WH, Chong CT, Chase HA (2018) Pyrolysis production of fruit peel biochar for potential use in treatment of palm oil mill effluent. J Environ Manag 213:400–408
35. Hashemian S, Salari K, Yazdi ZA (2014) Preparation of activated carbon from agricultural wastes (almond shell and orange peel) for adsorption of 2-pic from aqueous solution. J Ind Eng Chem 20:1892–1900
36. Lam SS, Liew RK, Wong YM et al (2017) Activated carbon for catalyst support from microwave pyrolysis of orange peel. Waste Biomass Valorization 8:2109–2119. https://doi.org/10.1007/s12649-016-9804-x
37. Brunauer S, Deming LS, Deming WE, Teller E (1940) On a theory of the van der waals adsorption of gases. J Am Chem Soc 62:1723–1732. https://doi.org/10.1021/ja01864a025